Published in final edited form as:
J Bone Miner Res. 2012 July ; 27(7): 1553–1565. doi:10.1002/jbmr.1600.

Claudin 18 is a novel negative regulator of bone resorption and osteoclast differentiation

Gabriel R. Linares, PhD[1,2], **Robert Brommage, PhD**[3], **David R. Powell, MD**[3], **Weirong Xing, PhD**[1,4], **Shin-Tai Chen, PhD**[1,5,6], **Fatima Z. Alshbool, Pharm.D**[1,7], **KH William Lau, PhD**[1,4,5], **Jon E. Wergedal, PhD**[1,4], and **Subburaman Mohan, PhD**[1,2,4,5]

[1]Musculoskeletal Disease Center, Jerry L. Pettis Memorial Veterans Affairs Medical Center, Loma Linda, CA 92357, USA

[2]Department of Physiology, Loma Linda University, Loma Linda, CA 92354, USA

[3]Lexicon Pharmaceuticals Inc., The Woodlands, TX 77381, USA

[4]Department of Medicine, Loma Linda University, Loma Linda, CA 92354, USA

[5]Department of Biochemistry, Loma Linda University, Loma Linda, CA 92354, USA

[6]Department of Microbiology, Loma Linda University, Loma Linda, CA 92354, USA

[7]Department of Pharmacology, Loma Linda University, Loma Linda, CA 92354, USA

Abstract

Claudin 18 (Cldn-18) belongs to a large family of transmembrane proteins that are important components of tight junction strands. Although several claudin members are expressed in bone, the functional role for any claudin member in bone is unknown. Here we demonstrate that disruption of Cldn-18 in mice markedly decreased total body bone mineral density, trabecular bone volume, and cortical thickness in *Cldn-18* $^{-/-}$ mice. Histomorphometric studies revealed that bone resorption parameters were increased significantly in *Cldn-18* $^{-/-}$ mice without changes in bone formation. Serum levels of TRAP5b and mRNA expression levels of osteoclast specific markers and signaling molecules were also increased. Loss of Cldn-18 further exacerbated calcium deficiency induced bone loss by influencing bone resorption, thereby resulting in mechanically weaker bone. *In vitro* studies with bone marrow macrophages revealed Cldn-18 disruption markedly enhanced RANKL-induced osteoclast differentiation but not MCSF-induced BMM proliferation. Consistent with a direct role for Cldn-18 in regulating osteoclast differentiation, overexpression of wild type but not PDZ binding motif deleted Cldn-18 inhibited RANKL-induced osteoclast differentiation. Furthermore, our findings indicate that Cldn-18 interacts with Zonula occludens 2 (ZO-2) to modulate RANKL signaling in osteoclasts. In conclusion, we demonstrate that Cldn-18 is a novel negative regulator of bone resorption and osteoclast differentiation.

Keywords

Tight junctions; claudin-18; osteoclasts; resorption; zonula occludens

Corresponding author and address for reprint requests: Subburaman Mohan, Ph.D., Musculoskeletal Disease Center (151), Jerry L. Pettis Memorial Veterans Affairs Medical Center, 11201 Benton Street, Loma Linda, CA 92357; Phone: (909) 825-7084 (ext 2932); Fax: (909) 796-1680; Subburaman.Mohan@va.gov.

Conflict of interest: R. Brommage and D. Powell are employees of Lexicon Pharmaceuticals Inc. and declare competing financial interests. G. Linares, W. Xing, S.T. Chen, F. Alshbool, K.H. Lau, J. Wergedal, and S. Mohan have nothing to declare.

Introduction

Osteoporosis poses a major public health threat not only in the United States but throughout the world. Osteoporosis is characterized by decreased bone mineral density and microarchitectural deterioration of bone tissue which result in the formation of porous bone (1). Normally, bone homeostasis is tightly regulated by a balance between bone formation and bone resorption. Disruption of this balance can lead to osteopenic diseases such as osteoporosis, which is caused by excessive bone resorption accompanied by a corresponding decrease in bone formation resulting in net bone loss (2). Because bone resorption rate is dependent on the number and activity of osteoclasts, it is important to understand the mechanisms that regulate osteoclast differentiation.

Osteoclasts are giant multi-nucleated cells that originate from hematopoietic cells of monocyte/macrophage lineage. These cells are involved in degrading mineralized bone matrix during bone resorption (3). It is well established that macrophage colony stimulating factor (MCSF) and receptor activator of nuclear factor kappa B ligand (RANKL) are necessary and sufficient for inducing osteoclast differentiation and function (4). Moreover, over the past several years a number of systemic and local factors have also been implicated in the regulation of osteoclast formation and function (5–9). However the role of other molecular components that regulate osteoclast differentiation remains to be determined. Therefore, it is critical to identify novel genes and their pathways that regulate osteoclast differentiation and functions. Such genes may interact with important osteoclast regulatory pathways such as MCSF, RANKL, or TNF-α signaling. Thus, the identification of other genes and their relative contribution to osteoclast regulation will advance our understanding of the key regulatory molecular pathways involved in osteoclast formation and function.

Tight junctions (TJs) are important in the development and maintenance of multi-cellular organisms because they aid in the assembly of cellular sheets. TJs are also critical for maintaining biological compartments and for keeping external and internal environments separate. Located at the apical region of the plasma membrane, TJs establish cell polarity by maintaining the polarized distribution of proteins and lipids. Canonical functions of TJs include regulating paracellular transport of ions, small molecules, and water. Besides their canonical function as a selective barrier, recent evidence demonstrates that TJs also participate in intracellular signaling pathways affecting cell proliferation, differentiation, and gene expression (10). These findings support an emerging role for TJs as dynamic regulators of cell functions beyond serving as a static fence or gate.

A major structural component of TJ strands is the Claudin (Cldn) family which consists of 24 members. Cldns encode 20–27 kDa proteins with four transmembrane domains, two extracellular loops, and a cytoplasmic C-tail. Certain Cldns are widely expressed at high levels suggesting a housekeeping function while others are expressed at low levels suggesting specialized or regulatory functions (11). The functional roles for several Cldn family members have been by identified by loss-of-function studies in mice. Ablation of Cldn-14, Cldn-1, and Cldn-5 affect cochlear hair cell function, and the skin and blood-brain barriers respectively (12–14). A severe renal phenotype is observed in mice lacking Cldn-7, Cldn-16, or Cldn-19, while Cldn-15 deficient mice exhibit megaintestine (15–18). Deletion of Cldn-11 hampers CNS nerve conduction and induces male sterility (19). Thus, the findings from loss of function studies clearly demonstrate that Cldns are crucial proteins in various biological systems.

Discrete phenotypes seen in mice with targeted disruption of different Cldns suggest that Cldns have highly specialized roles in particular cell types. Although, recent studies have shown that several Cldn family members are expressed in bone (20–23), their exact

biological function in bone biology remains unknown. In this regard, a high-throughput screen to analyze the functions of over 4500 genes by Lexicon Pharmaceuticals revealed that knockout of Cldn-18 resulted in reduced peak bone mass, with body vBMD and midshaft femur cortical thickness values 3 standard deviations below normal. This surprisingly large effect of Cldn-18 knockout suggested that it had an important role in bone. Since the function of any Cldn member in bone has not been identified, we undertook studies to characterize the skeletal phenotype of Cldn-18 knockout mice and determine the mechanism for reduced bone mass in the knockout mice.

Materials and Methods

Mice

Cldn-18 deficient (*Cldn-18* $^{-/-}$) mice were generated via targeted disruption of coding exons 2–4 of the murine homolog of the Cldn-18 gene (GenBank accession no. NM_019815) by homologous recombination in 129SvEvBrd-derived embryonic stem (ES) cells using the λ KO shuttle system as described (24). Genotyping of mice was accomplished using WT and mutant specific primers (Supplementary Table 1) for PCR. Littermate controls were used for all experiments. Mice were housed at Lexicon Pharmaceuticals Inc. (The Woodlands, TX) or Jerry L. Pettis Memorial VA Medical Center Veterinary Medical Unit (Loma Linda, CA) under standard approved laboratory conditions. Animal use protocols were approved by the Institutional Animal Care and Use Committee of the participating institutions. The *Claudin 18* $^{-/-}$ mice were produced in collaboration between Genentech, Inc. and Lexicon Pharmaceuticals, Inc. to analyze the function of secreted and transmembrane proteins.

Dietary calcium deficiency

Sixteen week old WT and *Cldn-18* $^{-/-}$ mice were fed a normal calcium diet or a low calcium diet. The normal calcium diet (TD97191, containing 0.6% calcium by weight) and the calcium deficient diet (TD95027, containing < 0.01% calcium by weight) were purchased from Harlan Teklad (Madison, WI). Mice were fed the indicated diet for 2 weeks.

Cell culture

Bone marrow stromal cells (BMSCs) were isolated from the femurs and the tibias of *Cldn-18* $^{-/-}$ mice and corresponding control mice as reported previously (25). Osteoblasts were obtained by collagenase digestion of newborn mouse calvaria as described (26). Primary osteoclast precursors or bone marrow macrophage (BMM) precursors were isolated from long bones (femur and tibia) of *Cldn-18* $^{-/-}$ and corresponding control mice (27) and maintained in α-MEM supplemented with 10% fetal bovine serum (FBS), penicillin (100 units/ml), streptomycin (100 μg/ml), and Macrophage Colony Stimulating Factor (MCSF) (25 ng/ml). MCSF was obtained from R&D Systems (Minneapolis, MN). Twenty-four hours later, non-adherent cells (BMMs) were collected and used for subsequent experiments. Osteoclasts were generated by incubating non-adherent-BMMs with MCSF (100 ng/ml) and Receptor activator of nuclear factor kappa B ligand (RANKL) (100 ng/ml) for 6 days. RANKL was obtained from R&D Systems (Minneapolis, MN). RAW264.7 cells (American Type Culture Collection, Manassas, VA), an osteoclast precursor cell line, were cultured in α-MEM containing 10% FBS, penicillin (100 units/ml), and streptomycin (100 μg/ml). All cells were maintained at 37°C in 5% CO_2.

Analysis of skeletal morphology

Dual energy x-ray absorption (DXA), Micro-computed tomography (μCT) analysis, and histomorphometry were carried out as previously reported (28).

Mechanical testing by 3-point bending

Femurs collected from WT and *Cldn-18* $^{-/-}$ mice fed a normal calcium or low calcium diet were tested using the Instron DynaMight testing system (Model 8840; Instron, Canton, MA) as described previously (29). Mechanical strength was determined by performing three point bending at the mid diaphysis as reported (30). Maximal load was defined as bending load at failure. Stiffness was calculated as the slope of the linear part of the load displacement curve.

ELISA

Serum levels of mouse osteocalcin (index of bone formation) and TRAP5b (index of osteoclast number) were measured according to the manufacturer's instructions (Immunodiagnostic systems, Fountain Hills, AZ). PTH serum levels were determined in mice fed normal calcium and low calcium diets using mouse intact PTH ELISA kit as per manufacturer's instructions (Immutopics Inc., San Clemente, CA).

Mineralized nodule formation

To induce differentiation, BMSCs were incubated with α-MEM containing 10% calf serum (CS), β-glycerophosphate (10 mM), and ascorbic acid (50 μg/ml) for 24 days. β-glycerophosphate and ascorbic acid were purchased from Sigma Aldrich (St. Louis, MO). Nodules were stained for mineralized matrix using alizarin red and mineralized area was quantified as described (31).

Gene expression analysis

Total RNA was extracted from isolated tissues or cells and synthesized into cDNA for real time RT-PCR analysis as previously described (25). Relative gene expression levels were examined and the housekeeping gene PPIA was used as an internal control in the PCR reaction. The fold change compared to control was calculated according to the formula $2^{-\Delta\Delta Ct}$. Primer sequences are listed in supplementary table 1.

Cloning of Claudin 18a2.1 and Claudin 18a2.1 ΔPDZ domain

Full length coding sequences of Claudin 18a2.1 and cytoplasmic tail containing PDZ binding motif truncated Claudin 18a2.1 (Cldn-18 ΔPDZ) were amplified by PCR with high fidelity enzyme Pfx50 (Invitrogen, Carlsbad, CA) using *Mus musculus* stomach cDNA as a template and cloned as described elsewhere (32). The primer sequences used were (5′ to 3′): Claudin 18a2.1 forward: GGGTCGACGCCACCATGTCGGTGACCGCCTGCCAGGGCTTGG; Claudin 18a2.1 reverse: CGCGGATCCCTACACATAGTCATACTTGGTAGGATGAG; and Cldn-18 ΔPDZ reverse: CGCGGATCCCTAGATGCACATCATCA. The cytoplasmic C-terminal deletion of PDZ binding motif of Cldn-18 (Cldn-18 ΔPDZ) was constructed by inserting a stop codon after the transmembrane domain resulting in termination at Ile-197. Claudin 18a2.1 and Cldn-18 ΔPDZ coding sequences were confirmed by DNA sequencing at Arizona State University (Tempe, AZ).

Murine leukemia virus-based viral vectors (MLV-based vector) production and transduction MLV-based vectors containing (β-gal, Claudin 18a2.1, or Cldn-18 ΔPDZ) were generated and RAW264.7 cells were transduced as previously described (33).

Lentivirus transduction

RAW264.7 cells were transduced with Mission® non-target shRNA control (Sigma-Aldrich, St. Louis, MO) transduction particles or five different Mission® ZO-2 transduction particles (ZO-2 shRNA 68–72) (Sigma-Aldrich, St. Louis, MO) as previously reported (32).

In vitro osteoclast formation

Tartrate resistant acid phosphatase (TRAP) stain was performed on primary non-adherent BMMs (WT and *Cldn-18* $^{-/-}$ mice) and RAW264.7 cells (untransduced, MLV-Cldn-18, MLV-β-gal, MLV-Cldn-18 ΔPDZ, non-target shRNA control, and ZO-2 shRNA). To induce osteoclast differentiation, non-adherent BMMs were incubated with MCSF (100 ng/ml) and RANKL (100 ng/ml) whereas RAW264.7 cells were incubated with only RANKL (30 ng/ml or 100 ng/ml) for 6 days or the indicated time periods. Osteoclastogenesis was evaluated by TRAP stain using Fast Garnet GBC sulfate salt (Sigma Aldrich, St. Louis, MO) as previously described (34). The number of multinucleated TRAP positive cells (defined as 3 or more nuclei per cell) was counted. Data are representative of 4 random fields per well.

Immunoblotting analysis

Stomach was obtained from WT and *Cldn-18* $^{-/-}$ mice and the gastric contents were emptied. Tissues were flash-frozen in liquid nitrogen and stored at −80°C until the extraction was performed. Briefly, the tissue was minced and homogenized in a tight-fitting glass homogenizer (using 30 strokes) with lysis buffer containing 50 mM Hepes (pH 7.4), 150 mM NaCl, 1.5 mM $MgCl_2$, 1 mM EGTA, 0.2% sodium deoxycholate, 0.05% SDS, 1% Triton X-100, and protease inhibitor cocktail (Sigma Aldrich, St. Louis, MO). Using a Sonic Dismembrator Model 100 (Fisher Scientific, Pittsburgh, PA) the stomach homogenate was briefly sonicated on ice and centrifuged at 5000 RPM for 5 minutes at 4°C to remove excess debris.

For preparation of whole cell lysates, BMMs derived from WT and *Cldn-18* $^{-/-}$ mice were washed two times with PBS. Following collection in cold PBS, cells were centrifuged at 425 x g for 5 minutes at 4°C and the resulting pellets were suspended in lysis buffer (described above). Samples were lysed under gentle rotation for 30 minutes at 4°C and were sonicated briefly on ice. The cell lysates were centrifuged at 12,000 x g for 10 minutes at 4°C to remove excess debris and the resulting supernatant was used for western blot analysis. Nuclear extracts of RAW264.7 cells expressing MLV-Cldn-18, MLV-Cldn-18 ΔPDZ, and MLV-β-Gal were prepared as reported elsewhere (35). Protein concentration was determined by Bradford method and immunoblotting was carried out as described (36). Membranes were probed with antibodies against Cldn-18 (C-term) (1:250) (Invitrogen, Carlsbad, CA), ZO-2 (R-19) (1:250) (Santa Cruz Biotechnology Inc, Santa Cruz, CA), Histone H3 (1:10,000) (Sigma Aldrich, St. Louis, MO), and β-actin (1:10,000) (Sigma Aldrich, St. Louis, MO).

Immunoprecipitation

MLV-Cldn-18 RAW264.7 cells were cross-linked as previously described (28). Cells were incubated in lysis buffer containing 10 mM HEPES (pH 7.4), 150 mM NaCl, 0.5% sodium deoxycholate, 0.2% SDS, 1% Triton X-100, and 1x protease inhibitor cocktail for 30 minutes on ice. Immunoprecipitation was performed using 2 μg of ZO-2 (R-19) specific polyclonal antibody (Santa Cruz Biotechnology Inc, Santa Cruz, CA) or control IgG as described elsewhere (28). The immunoprecipitated proteins were separated by SDS-PAGE under reducing conditions for immunoblot and probed with polyclonal antibody against Claudin 18 (C-term) (1:250) (Invitrogen, Carlsbad, CA).

Preosteoclast adhesion assay

Non-adherent BMMs were plated in 6-well culture dishes in α-MEM containing 10% FBS and 25 ng/ml MCSF at a density of 0.5 X 10^6 cells/well. Following a 60 minute incubation, non-adherent cells were gently washed away with PBS and adherent cells were fixed after 2 hrs, stained with 0.1% crystal violet and counted.

Analysis of number of nuclei per osteoclast in tibia

The number (N) of nuclei per osteoclast in TRAP stained sections of the secondary spongiosa of proximal tibia in WT and *Cldn-18* $^{-/-}$ mice at 4 weeks of age was determined as previously described (37). Briefly, twenty osteoclasts per sample were randomly selected with operator blinded, before osteoclasts were sorted based on 1–2 and 3–6 N.Nuclei per osteoclast.

Cell proliferation

CyQUANT assay was used to determine cell proliferation and was performed as per the manufacturer's instructions (Invitrogen, Carlsbad, CA). BMMs isolated from WT and *Cldn-18* $^{-/-}$ mice were treated with MCSF (1 ng/ml, 10 ng/ml, and 100 ng/ml) for 48 hours and cell proliferation was determined.

Cignal™ lenti reporter assay

Non-target shRNA and ZO-2 shRNA RAW264.7 cells were transduced with Cignal™ lenti reporters (NF-κB, NFATc1, AP-1, or SMAD) as per the manufacturer's instructions (SABiosciences, Frederick, MD) to assess transcriptional activity. Cells were incubated in the presence of RANKL (30 ng/ml) for 12 hours followed by ONE-GLO Luciferase assay (Promega, Madison, WI).

Statistical analysis

Results are expressed as means ± SD (standard deviation) and were analyzed using Student's T-test or ANOVA (one-way or two way) (Statistica 6, Tulsa, OK) as appropriate. Post-hoc analysis was performed using Duncan's test. Values were considered statistically significant when $P < 0.05$.

Results

Generation of Cldn-18 $^{-/-}$ mice

A high throughput screen to analyze the function of over 4500 genes revealed that knockout of Cldns 2, 6, 8, and 14 yielded no apparent skeletal phenotypes while knockout of Cldn-1 was neonatal lethal. The disruption of Cldn-18 resulted in a significant reduction of peak bone mass and therefore, we focused our efforts on investigating the consequence of Cldn-18 disruption on the skeletal phenotype and the mechanism of Cldn-18 action in regulating peak bone mass. *Cldn-18* $^{-/-}$ mice were generated using conventional gene targeting (24). Cldn-18 was inactivated by replacing exons 2–4 with LacZ/neomycin selection cassette and Southern blotting confirmed disruption of Cldn-18 gene (Supplementary Fig. 1A,B). Genotyping of genomic DNA from heterozygous (+/−), *Cldn-18*-null homozygous (−/−), and wild type (+/+) reveal the presence of a 453-bp and 551-bp product from WT and mutant alleles respectively (Supplementary Fig. 1C). Cldn-18 deficiency was confirmed in stomach (positive control) and bone marrow macrophages (BMMs) from *Cldn-18* $^{-/-}$ mice by immunoblot (Supplementary Fig. 1D). Mating of Cldn-18 heterozygous mice generated pups of three possible genotypes (+/+, +/−, and −/−) at the expected Mendelian frequency (+/+ = 61; +/− = 127; and −/− = 58) and all were viable. Homozygous *Cldn-18* $^{-/-}$ mice exhibited no obvious differences compared to control littermates in a battery of tests designed to detect developmental, behavioral, metabolic, ophthalmic, and hematologic abnormalities However, *Cldn-18* $^{-/-}$ mice exhibited histologic abnormalities in the gastric mucosa marked by the presence of inflammatory infiltrates and decreased numbers of well-differentiated gastric chief cells and parietal cells. These findings are consistent with a recent report describing atrophic gastritis in *Cldn-18* $^{-/-}$ mice (38).

BMD is reduced in Cldn-18 $^{-/-}$ mice

Body length and femur length were unaffected between *Cldn-18* $^{-/-}$ mice and littermate controls (data not shown). Whole body DXA revealed reductions of 20%–25% in total body bone mineral content (BMC), total body bone mineral density (BMD), vertebra BMD, and femur BMD in *Cldn-18* $^{-/-}$ mice compared to control mice at 26 weeks of age (Fig. 1A–D). Phenotypic differences due to gender-genotype interaction were not observed and therefore data from both genders were pooled for analysis. MicroCT analysis revealed that *Cldn-18* $^{-/-}$ mice had decreased (20%) cortical bone thickness relative to littermate control mice at 26 weeks of age (Fig. 1F). Cross-sectional area (and hence diameter) was not significantly different between the two groups (Fig. 1E). Trabecular bone volume, trabecular thickness, and trabecular number were dramatically reduced by 50% in *Cldn-18* $^{-/-}$ mice (Fig. 1G–I, K) while trabecular separation was increased by 50% compared to control mice at 26 weeks of age (Fig. 1J). Connectivity density was reduced 50% in *Cldn-18* $^{-/-}$ mice (Fig. 1L) and this group also displayed a higher ratio of rods to plates as indicated by structure model index (SMI) (Fig. 1M). Similar deficits were also observed in mice at 4 weeks (Supplementary Fig. 2). Significant perturbations in levels of calcium, phosphate, glucose, albumin, creatinine, and cholesterol were not observed in *Cldn-18* $^{-/-}$ mice compared to wild type mice (Supplementary Fig. 3). This finding indicates that a systemic deficiency of ions or nutrients is not the cause for decreased BMD in *Cldn-18* $^{-/-}$ mice.

Bone formation is unaffected by Cldn-18 deficiency

Dynamic histomorphometry at trabecular bone of the secondary spongiosa of the proximal tibia revealed that bone formation parameters were not significantly different between *Cldn-18* $^{-/-}$ and control mice at 4 weeks of age (Fig. 2A–D). In addition, serum levels and bone mRNA expression of osteocalcin, a bone formation marker, were unaltered between *Cldn-18* $^{-/-}$ mice and control mice (Fig. 2E,F). Moreover, *in vitro* bone formation assay using bone marrow stromal cells from *Cldn-18* $^{-/-}$ and control mice demonstrated no significant difference in mineralized nodule formation (Fig. 2G,H). Collectively, these results indicate that Cldn-18 deficiency does not impair bone formation.

Cldn-18 deficiency increases bone resorption and osteoclast differentiation

In contrast, TRAP staining revealed an 87% increase in TRAP labeled osteoclast surface in the trabecular bone of secondary spongiosa of the proximal tibia of *Cldn-18* $^{-/-}$ mice relative to control mice (Fig. 3A,B) as well as increased osteoclast number (Fig. 3C). The number of TRAP positive osteoclasts containing 3–6 nuclei was greater while the number of TRAP positive osteoclasts containing 1–2 nuclei was lower in *Cldn-18* $^{-/-}$ mice compared to WT mice (Fig. 3D). Serum levels of TRAP5b, a marker of osteoclast number, were elevated (41%) in *Cldn-18* $^{-/-}$ mice and correlated negatively with femur trabecular BV/TV (Fig. 3G,H). Consistent with these data, mRNA expression of TRAP and cathepsin K (Ctsk) (Fig. 3E,F) were increased 88% and 69% respectively in the femurs of *Cldn-18* $^{-/-}$ mice. Osteoclast progenitor cells derived from *Cldn-18* $^{-/-}$ mice and treated with RANKL formed 80% more multinucleated TRAP positive cells than WT mice *in vitro* (Fig. 3I,J). To determine if the differences in the number of osteoclasts formed using BMMs-derived from WT and *Cldn-18* $^{-/-}$ mice are due to differences in adhesion of osteoclast precursors, we measured MCSF-mediated preosteoclast adhesion using non-adherent BMMs-derived from the two strains of mice. We found no significant difference between the two genotypes in the preosteoclast adhesion assay (Fig. 3K). We also found that loss of Cldn-18 did not significantly influence the size of TRAP positive multinucleated osteoclasts formed using MCSF and RANKL treatment of BMMs (Fig. 3L). Furthermore, neither the number of nuclei per osteoclast nor the distribution of nuclei in the osteoclast preparations was different between the two genotypes (data not shown). Together these findings demonstrate

that lack of Cldn-18 increases osteoclast formation and that increased bone resorption is the major cause for decreased BMD in *Cldn-18* $^{-/-}$ mice.

Calcium deficiency induced bone loss is exacerbated in Cldn-18 $^{-/-}$ mice

Calcium deficiency induces bone loss via a mechanism involving increased bone resorption (39). To evaluate whether calcium deficiency exaggerates bone loss in mice lacking Cldn-18 gene, WT and *Cldn-18* $^{-/-}$ mice were subjected to a normal calcium or low calcium diet for 2 weeks. DXA revealed BMD was reduced by 13, 14, and 31% at whole body, femur, and lumbar respectively in calcium deficient WT mice (Fig. 4A). As expected, BMD was also reduced by 15, 13, and 27% in *Cldn-18* $^{-/-}$ mice relative to WT normal calcium treated mice. However, calcium depletion in *Cldn-18* $^{-/-}$ mice resulted in further skeletal deficits (Fig. 4A). Gene-diet interaction was significant for lumbar BMD ($P < 0.05$). To evaluate whether the combination of calcium deficiency and loss of Cldn-18 compromises bone quality, μCT analysis of L5 vertebra was performed. BV/TV was reduced by 42% in the low calcium diet *Cldn-18* $^{-/-}$ mice compared to 21% in the *Cldn-18* $^{-/-}$ mice fed normal calcium diet (Fig. 4B). Trabecular thickness was reduced 24% in the low calcium diet *Cldn-18* $^{-/-}$ mice compared to 10% in the *Cldn-18* $^{-/-}$ mice normal calcium diet group (Fig. 4B). Trabecular number was decreased 30% in the low calcium diet *Cldn-18* $^{-/-}$ mice compared to 16% in the *Cldn-18* $^{-/-}$ mice normal calcium diet group while trabecular separation was increased 40% in the low calcium diet *Cldn-18* $^{-/-}$ mice relative to 18% in the *Cldn-18* $^{-/-}$ mice normal calcium diet group (Fig. 4B). Dynamic histomorphometry at trabecular bone of the secondary spongiosa of distal femurs demonstrated that BFR and MAR were unaffected by 2 week calcium depletion in both WT and *Cldn-18* $^{-/-}$ mice (Fig. 4C,D), whereas % TRAP labeled osteoclast surface was markedly increased in low calcium diet *Cldn-18* $^{-/-}$ mice compared to normal calcium *Cldn-18* $^{-/-}$ mice and low calcium WT groups (Fig. 4E). Accordingly, serum levels of PTH in the normal calcium *Cldn-18* $^{-/-}$ mice were further increased by calcium deficiency (Fig. 4F). As expected measurements of bone breaking strength and stiffness were significantly decreased by combined deficiency of Cldn-18 and calcium compared to either deficiency alone (Fig. 4G,H). Collectively, these findings demonstrate that calcium depletion in *Cldn-18* $^{-/-}$ mice further exacerbates bone loss and reduces bone strength.

Cldn-18 influences the formation of osteoclasts

Cldn-18 was identified as a downstream target gene for the T/EBP/NKX2.1 homeodomain transcription factor in the lung (40). Alternative splicing of Cldn-18 gene resulted in two tissue-specific isoforms, Cldn-18a1 (lung isoform) and Cldn-18a2 (stomach isoform) driven by alternate promoters and results in 4 different isoforms (Cldn-18a1.1, a1.2, a2.1, and a2.2) (Fig. 5A) (40). Cldn-18 is also known to be expressed in a variety of other tissues and cell types including the esophagus, inner ear, hair follicles, and radial glia (41,42). Of the various Cldn-18 isoforms, stomach specific isoform Cldn 18a2.1 was predominantly expressed in bone tissue as well as in isolated bone cells (Fig. 5B). The consequence of Cldn-18 overexpression (Cldn-18a2.1 isoform) on the formation of multinucleated TRAP positive cells was evaluated using RAW264.7 cells. Cldn-18 overexpression was confirmed by real time RT-PCR and western blot (data not shown). RANKL induced osteoclastogenesis was dramatically inhibited in Cldn-18 overexpressing cells (Fig. 5C,D). Consistent with reduced osteoclast formation, RANKL stimulation of Ctsk expression was markedly decreased in Cldn-18 overexpressing cells (Fig. 5E). Several Cldns including Cldn-18 end in a PDZ binding motif capable of binding to PDZ domain containing proteins (43–45). To determine the role of PDZ binding motif in mediating Cldn-18 biological effects, we evaluated the effects of overexpression of mutant Cldn-18 lacking cytoplasmic C-terminal PDZ binding motif on RANKL-induced osteoclast differentiation (Supplementary Fig. 4). In contrast to

intact Cldn-18, overexpression of mutant Cldn-18 in RAW264.7 cells did not affect RANKL induced formation of multinucleated TRAP positive osteoclasts (Fig. 5F,G).

To determine if Cldn-18 deficiency influences tight junction function, we measured ^{45}Ca transport across monolayers of RAW264.7 cells overexpressing Cldn-18 or β–Gal on permeable filter supports. Transport data was estimated from the amount of ^{45}Ca transported to lower compartment at different times. No significant difference was found in ^{45}Ca transport (Supplementary Fig. 5). These results suggest that Cldn-18 may be a negative regulator of osteoclast differentiation and that increased bone resorption in *Cldn-18* $^{-/-}$ mice is a direct consequence of decreased Cldn-18 action on osteoclast formation.

Cldn-18 regulates RANKL not MCSF signaling in osteoclasts

MCSF and RANKL are necessary and sufficient for inducing osteoclast differentiation (4,46). To determine if the increased bone resorption in *Cldn-18* $^{-/-}$ mice is due to increased proliferation or differentiation of osteoclast precursors, we examined gene expression levels of osteoclast progenitors and mature osteoclasts. The mRNA levels of osteoclast differentiation markers (TRAP, Ctsk, and calcitonin receptor) and signaling molecules involved in regulating osteoclast differentiation and function (MitF, NFATc1, c-Fos, and c-Src) were significantly increased in the femurs of *Cldn-18* $^{-/-}$ mice (Fig. 6A,B). In contrast, the expression of markers for osteoclast progenitors (Cd11b, Csf1r, and PU-1), proliferation (Cyclin D1), and apoptosis (Bcl2l11) were unchanged (Fig. 6A). Consistent with these data, deletion of Cldn-18 did not affect MCSF induced osteoclast precursor cell proliferation (Fig. 6C), suggesting that increased bone resorption in *Cldn-18* $^{-/-}$ mice is not due to altered proliferation. Furthermore, expression of Cyclin D1, RANK, TRAP, and Ctsk in BMMs was not significantly different in MCSF treated BMMs from *Cldn-18* $^{-/-}$ mice and control mice (Fig. 6D). In contrast, stimulation with RANKL markedly increased TRAP and Ctsk expression in *Cldn-18* $^{-/-}$ osteoclast precursors compared to WT mice (Fig. 6E). These data indicate that Cldn-18 may differentially regulate osteoclast differentiation via RANKL signaling pathway.

Zonula Occludens-2 (ZO-2) binds to Cldn-18 and modulates RANKL signaling in osteoclasts We next tested whether Cldn-18 effects on RANKL signaling are mediated in part via interaction of PDZ domain of Cldn-18 with PDZ domain containing protein, zonula occludens (ZO)-2, since certain Cldns interact with ZO proteins (44,47) and ZO-2 is highly expressed in osteoclasts (data not shown). Accordingly, an interaction between Cldn-18 and ZO-2 was detected by immunoprecipitation (Fig. 6F). Numerous studies have demonstrated ZO-2 contains a nuclear localization signal and that ZO-2 nuclear translocation is associated with increased gene expression (48–52). Because Cldn-18 interacted with ZO-2, we predicted that Cldn-18 overexpression would reduce RANKL induced nuclear translocation of ZO-2. Accordingly, Cldn-18 overexpression in RAW264.7 cells decreased ZO-2 nuclear localization by 58 ± 21% ($P<0.05$) compared to MLV-β-Gal control cells (Fig. 6G). In contrast, overexpression of mutant Cldn-18 with deletion of C-terminal PDZ binding motif did not influence nuclear localization of ZO-2 (91 ± 13% of β-gal group, n=3) in the presence of RANKL (Fig. 6H). To assess whether ZO-2 is an important mediator of Cldn-18 effects on osteoclast differentiation, we examined the consequence of ZO-2 inhibition on osteoclast differentiation by utilizing lentiviral shRNA. RANKL induced osteoclast formation was dramatically reduced 50% in ZO-2 shRNA cells relative to non-target shRNA (Fig. 6I,J). Consistent with reduced osteoclast formation, TRAP and Ctsk expression was significantly reduced in ZO-2 shRNA cells following RANKL stimulation (Fig. 6K). These findings indicate that Cldn-18 interacts with ZO-2 to modulate RANKL signaling in osteoclasts.

It is well established that NF-κB, NFAT, and AP-1 are important transcription factors in modulating RANKL induced osteoclast differentiation (4). Therefore, the consequence of ZO-2 inhibition on RANKL induced activation of osteoclast specific transcription factors was examined. As expected, transcriptional activation of NF-κB, NFAT, and AP-1 in RAW264.7 cells treated with control shRNA increased robustly in response to RANKL treatment. In contrast, RANKL induced NF-κB and NFAT promoter activity was dramatically reduced in ZO-2 shRNA cells whereas AP-1 activity was unaffected (Fig. 6L). The specificity of the reporter assay was confirmed by evaluating SMAD activity since it does not respond strongly to RANKL stimulation. These results suggest that RANKL stimulation of NF-κB and NFAT transcriptional activity is in part mediated by ZO-2.

Discussion

A high throughput screen of knockout mouse phenotypes identified a new functional role for Cldn-18, a TJ protein, in bone. We provide the first experimental evidence for a Cldn family member in regulating RANKL mediated osteoclast differentiation and thereby bone resorption. Consistent with an important role for Cldns in bone, a sequence variant in Cldn-14 was associated with decreased bone mineral density in humans (53). These findings raise the possibility that Cldns may serve an important function in bone biology and warrants further investigation.

We examined whether the increased bone resorption in *Cldn-18* $^{-/-}$ mice was due to increased proliferation or increased differentiation of osteoclast precursors, and found that deletion of Cldn-18 did not affect MCSF signaling. In the presence of RANKL, we observed a robust increase in osteoclast specific gene expression, suggesting that Cldn-18 may differentially regulate osteoclast differentiation via RANKL signaling. It is unknown whether Cldn-18 regulates RANKL independent actions. Future studies will evaluate the effects of factors that are known to regulate osteoclast formation (TNF-α, prostaglandins, interleukins) (54,55) besides RANKL in order to determine if Cldn-18 can also regulate osteoclast differentiation via a RANKL independent mechanism.

Our findings provide the first evidence that Cldn-18 is expressed in osteoclasts and affects bone mineral density by regulating bone resorption. Relatively little is known about the role of TJ proteins in osteoclasts and little is known on the role of any Cldn family member in bone. There is some evidence to suggest that gap junctions are important in skeletal biology (56). Studies by Civitelli and colleagues have shown that disruption of connexin 43, a major gap junction protein, leads to decreased bone mineral density in mice (57). Moreover, connexin 43 participates in the fusion of osteoclast precursors into mature osteoclasts (58). However, it remains to be determined whether Cldn-18 interacts with connexin proteins and whether Cldn-18 disruption affects gap junctions in bone. Occludin is a transmembrane protein that is also a component of the TJ. Disruption of occludin in mice leads to a thinning of cortical bone and postnatal growth retardation (59). In *Cldn-18* $^{-/-}$ mice, differences in growth rate were not observed, thus suggesting that different mechanisms may regulate occludin and Cldn-18 actions in bone.

Previously, we found two weeks of a low calcium diet caused serum calcium deficit, increased serum PTH levels and bone resorption rate in WT mice (30). The PTH effect on osteoclast recruitment is also known to be mediated via activation of the RANKL pathway (39). Consistent with the prediction that Cldn-18 interacts with RANKL signaling to regulate osteoclast differentiation, we found that bone loss-induced by calcium deficiency was exacerbated in *Cldn-18* $^{-/-}$ mice compared to WT mice, thus suggesting that the increased bone resorption is the cause for greater bone loss in calcium deficient *Cldn-18* $^{-/-}$

mice. Future studies will elucidate the molecular mechanism by which Cldn-18 deficiency interacts with calcium deficiency to increase bone resorption.

The unexpected function of Cldn-18 in regulating bone resorption suggests that Cldn-18 exerts other functions besides regulating paracellular transport. It has been reported that PDZ domain containing proteins such as ZO-1, ZO-2, and ZO-3 bind to the YV sequence in the carboxy terminus of Cldn proteins (44). Of these three proteins, we focused on ZO-2 because knockout of ZO-2 is embryonically lethal (60) and ZO-2 expression was highest in osteoclasts. As transmembrane proteins, the interaction of Cldns with the actin based cytoskeleton via membrane associated proteins (such as ZO proteins) is important for maintaining structural organization of the junctional complex at the plasma membrane and for signal transduction (61). In terms of the molecular mechanism for Cldn-18 action, we predict that ZO-2 mediates Cldn-18 action by signaling to and from the TJ. Overexpression of deleted C-terminal PDZ binding motif from Cldn-18 in RAW264.7 cells did not affect ZO-2 nuclear levels nor osteoclast differentiation following RANKL stimulation. These findings indicate that the PDZ binding motif is important in mediating the inhibitory effects of Cldn-18 on ZO-2 nuclear localization and osteoclast differentiation, and provide experimental evidence for involvement of the interaction between Cldn-18 and PDZ domain proteins (e.g. ZO-2) in regulating Cldn-18 signaling. Together, these results point to an important role for the C-terminal PDZ binding motif in mediating Cldn-18 biological effects on the regulation of RANKL-induced osteoclast differentiation.

TJs have also been shown to regulate gene expression via interactions with ZO-1-ZO-3 and MUPP1 (52). For example ZO-2 modulates the transcriptional activity of AP-1 and cyclin D promoters (50,51). These findings suggest that ZO-2 may function to regulate the activity of transcription factors. In our study we observed that RANKL treatment induced the localization of ZO-2 to the nucleus and that overexpression of Cldn-18 abrogated this effect. In addition, we found that ZO-2 modulated the activity of NFATc1 and NF-κB, important transcription factors involved in RANKL induced osteoclast differentiation. Therefore, it is possible that ZO-2 may potentially mediate the effects of Cldn-18 in osteoclasts by interacting with these transcription factors. Future studies will examine the involvement of ZO-2 as a potential intracellular mediator of Cldn-18 effects in osteoclasts. In addition, basal mRNA levels of osteoclast transcription factors and signaling molecules (MitF, NFATc1, c-Fos, and c-Src) were elevated in the bones of *Cldn-18* $^{-/-}$ mice, thereby suggesting that Cldn-18 may mediate its effects on osteoclast differentiation in part by interacting with these pathways. Future studies to further identify and characterize the molecular pathway by which Cldn-18 acts will advance our understanding on the regulation of osteoclast differentiation.

In terms of mechanism for Cldn action in bone, canonical functions of TJs include regulating paracellular transport of ions, small molecules, and water. We found that serum levels of calcium and phosphate, important ions of bone metabolism, were unchanged by Cldn-18 disruption. Furthermore, Cldn-18 overexpression did not alter the paracelluar transport of calcium, thereby suggesting that Cldn-18 disruption does not influence paracellular transport in osteoclasts. The loss of ZO-2 reduced the stimulatory effect of RANKL on osteoclast differentiation and gene expression suggesting an unexpected function of ZO-2 in regulating osteoclast differentiation. Our data suggests that Cldn-18 modulates RANKL induced osteoclast differentiation via a mechanism that is independent of its TJ function. These data are consistent with others who have reported an emerging role for TJ proteins as dynamic regulators of cell functions (proliferation, differentiation, and gene expression) (10).

Although Cldns are broadly expressed in multiple tissues, ablation of particular Cldns in certain tissues can lead to discrete phenotypic changes (12–14,18,62) suggesting that Cldns exhibit both redundant and specific physiological functions. Our *in vitro* data suggests that Cldn-18 exerts a direct effect on osteoclast differentiation. Because Cldn-18 was globally disrupted and Cldn-18 is expressed in other tissues besides bone, we cannot exclude the possibility that the phenotype of *Cldn-18* $^{-/-}$ mice could also be mediated in part by disruption of Cldn-18 in other tissues. In this regard, Hayashi and colleagues (38) recently showed that global disruption of Cldn-18 in mice resulted in the development of atrophic gastritis. Cldn-18 deficiency led to a pathological increase in the expression of the inflammatory markers IL-1β, TNF-a, and COX-2 in the stomach, as well as elevated serum levels of IL-1β (38). Based on these findings, we cannot definitively rule out the possibility that gastric abnormalities and/or increased levels of inflammatory markers also contribute to the increased osteoclast differentiation/bone resorption observed in the present study. Future studies to determine the role of local Cldn-18 in bone using conditional KO will elucidate any differences between a total versus local knockout.

In conclusion, we demonstrate that Cldn-18 is a novel negative regulator of bone resorption. Our results established a critical role for Cldn-18 in regulating osteoclast differentiation both *in vitro* and in bones. Additionally, we found that Cldn-18 interacts with ZO-2 and that Cldn-18 effects on osteoclast differentiation are mediated in part by ZO-2. Understanding the osteoclast differentiation process is important because the pathogenesis of bone diseases such as osteoporosis is characterized by abnormal osteoclastogenesis. Therefore, it is possible that Cldn-18 related disruption in osteoclasts could contribute to development of skeletal disease. Future studies investigating the molecular mechanisms of Cldn-18 action in bone may prove useful in developing therapeutic strategies for the prevention and treatment of low bone mass.

Supplementary Material

Refer to Web version on PubMed Central for supplementary material.

Acknowledgments

The authors would like to thank Jeff Liu (Lexicon Pharmaceuticals Inc), Catrina Alarcon, Anil Kapoor, Joe Rung-Aroon, and Sheila Pourteymoor for their expert technical assistance. The screening, generation, and phenotypic characterization of *Cldn-18* $^{-/-}$ mice was accomplished at Lexicon Pharmaceuticals Inc. in The Woodlands, TX. All other work was performed with the facilities provided by the Department of Veterans Affairs in Loma Linda, CA. This work was supported by National Institutes of Health grants R01AR31062 (S.M.), 1F31AR056204 (G.R.L.), and 5R25GM060507 (Loma Linda University Center for Health Disparities and Molecular Medicine).

G.R.L., W.X., F.A., K.H.L., and S.M. designed experiments and performed data analysis and interpretation. G.R.L. performed experiments and composed the manuscript with assistance from S.M. R.B. and D.P. generated *Cldn-18* $^{-/-}$ mice and characterized the phenotype. S.C. performed viral vector preparation and transduction and J.E.W. performed dynamic histomorphometry and histology experiments. All authors provided critical revisions for the manuscript. S.M. conceived and oversaw the entire the project.

Grant support: National Institute of Heath grants R01AR31062, 1F31AR056204, and 5R25GM060507.

References

1. Clowes JA, Riggs BL, Khosla S. The role of the immune system in the pathophysiology of osteoporosis. Immunol Rev. 2005; 208:207–227. [PubMed: 16313351]
2. Kawai M, Mödder UI, Khosla S, Rosen CJ. Emerging therapeutic opportunities for skeletal restoration. Nat Rev Drug Discov. 2011; 10(2):141–156. [PubMed: 21283108]
3. Reddy SV. Regulatory mechanisms operative in osteoclasts. Crit Rev Eukaryot Gene Expr. 2004; 14(4):255–270. [PubMed: 15663356]

4. Boyle WJ, Simonet WS, Lacey DL. Osteoclast differentiation and activation. Nature. 2003; 423(6937):337–342. [PubMed: 12748652]
5. Raisz LG. Pathogenesis of osteoporosis: concepts, conflicts, and prospects. J Clin Invest. 2005; 115(12):3318–3325. [PubMed: 16322775]
6. Ross FP. Cytokine regulation of osteoclast formation and function. J Musculoskelet Neuronal Interact. 2003; 3(4):282–286. discussion 292–284. [PubMed: 15758299]
7. Kearns AE, Khosla S, Kostenuik PJ. Receptor activator of nuclear factor kappaB ligand and osteoprotegerin regulation of bone remodeling in health and disease. Endocr Rev. 2008; 29(2):155–192. [PubMed: 18057140]
8. Lorenzo J, Horowitz M, Choi Y. Osteoimmunology: interactions of the bone and immune system. Endocr Rev. 2008; 29(4):403–440. [PubMed: 18451259]
9. Novack DV, Teitelbaum SL. The osteoclast: friend or foe? Annu Rev Pathol. 2008; 3:457–484. [PubMed: 18039135]
10. Matter K, Balda MS. Epithelial tight junctions, gene expression and nucleo-junctional interplay. J Cell Sci. 2007; 120(Pt 9):1505–1511. [PubMed: 17452622]
11. Van Itallie CM, Anderson JM. Claudins and epithelial paracellular transport. Annu Rev Physiol. 2006; 68:403–429. [PubMed: 16460278]
12. Ben-Yosef T, Belyantseva IA, Saunders TL, Hughes ED, Kawamoto K, Van Itallie CM, Beyer LA, Halsey K, Gardner DJ, Wilcox ER, Rasmussen J, Anderson JM, Dolan DF, Forge A, Raphael Y, Camper SA, Friedman TB. Claudin 14 knockout mice, a model for autosomal recessive deafness DFNB29, are deaf due to cochlear hair cell degeneration. Hum Mol Genet. 2003; 12(16):2049–2061. [PubMed: 12913076]
13. Furuse M, Hata M, Furuse K, Yoshida Y, Haratake A, Sugitani Y, Noda T, Kubo A, Tsukita S. Claudin-based tight junctions are crucial for the mammalian epidermal barrier: a lesson from claudin-1-deficient mice. J Cell Biol. 2002; 156(6):1099–1111. [PubMed: 11889141]
14. Nitta T, Hata M, Gotoh S, Seo Y, Sasaki H, Hashimoto N, Furuse M, Tsukita S. Size-selective loosening of the blood-brain barrier in claudin-5-deficient mice. J Cell Biol. 2003; 161(3):653–660. [PubMed: 12743111]
15. Tatum R, Zhang Y, Salleng K, Lu Z, Lin JJ, Lu Q, Jeansonne BG, Ding L, Chen YH. Renal salt wasting and chronic dehydration in claudin-7-deficient mice. Am J Physiol Renal Physiol. 2010; 298(1):F24–34. [PubMed: 19759267]
16. Kausalya PJ, Amasheh S, Günzel D, Wurps H, Müller D, Fromm M, Hunziker W. Disease-associated mutations affect intracellular traffic and paracellular Mg2+ transport function of Claudin-16. J Clin Invest. 2006; 116(4):878–891. [PubMed: 16528408]
17. Miyamoto T, Morita K, Takemoto D, Takeuchi K, Kitano Y, Miyakawa T, Nakayama K, Okamura Y, Sasaki H, Miyachi Y, Furuse M, Tsukita S. Tight junctions in Schwann cells of peripheral myelinated axons: a lesson from claudin-19-deficient mice. J Cell Biol. 2005; 169(3):527–538. [PubMed: 15883201]
18. Tamura A, Kitano Y, Hata M, Katsuno T, Moriwaki K, Sasaki H, Hayashi H, Suzuki Y, Noda T, Furuse M, Tsukita S. Megaintestine in claudin-15-deficient mice. Gastroenterology. 2008; 134(2): 523–534. [PubMed: 18242218]
19. Gow A, Southwood CM, Li JS, Pariali M, Riordan GP, Brodie SE, Danias J, Bronstein JM, Kachar B, Lazzarini RA. CNS myelin and sertoli cell tight junction strands are absent in Osp/claudin-11 null mice. Cell. 1999; 99(6):649–659. [PubMed: 10612400]
20. Wongdee K, Pandaranandaka J, Teerapornpuntakit J, Tudpor K, Thongbunchoo J, Thongon N, Jantarajit W, Krishnamra N, Charoenphandhu N. Osteoblasts express claudins and tight junction-associated proteins. Histochem Cell Biol. 2008; 130(1):79–90. [PubMed: 18365232]
21. Hatakeyama N, Kojima T, Iba K, Murata M, Thi MM, Spray DC, Osanai M, Chiba H, Ishiai S, Yamashita T, Sawada N. IGF-I regulates tight-junction protein claudin-1 during differentiation of osteoblast-like MC3T3-E1 cells via a MAP-kinase pathway. Cell Tissue Res. 2008; 334(2):243–254. [PubMed: 18855015]
22. Wongdee K, Riengrojpitak S, Krishnamra N, Charoenphandhu N. Claudin expression in the bone-lining cells of female rats exposed to long-standing acidemia. Exp Mol Pathol. 2010; 88(2):305–310. [PubMed: 20035748]

23. Prêle CM, Horton MA, Caterina P, Stenbeck G. Identification of the molecular mechanisms contributing to polarized trafficking in osteoblasts. Exp Cell Res. 2003; 282(1):24–34. [PubMed: 12490191]
24. Salojin KV, Owusu IB, Millerchip KA, Potter M, Platt KA, Oravecz T. Essential role of MAPK phosphatase-1 in the negative control of innate immune responses. J Immunol. 2006; 176(3):1899–1907. [PubMed: 16424221]
25. Govoni KE, Lee SK, Chadwick RB, Yu H, Kasukawa Y, Baylink DJ, Mohan S. Whole genome microarray analysis of growth hormone-induced gene expression in bone: T-box3, a novel transcription factor, regulates osteoblast proliferation. Am J Physiol Endocrinol Metab. 2006; 291(1):E128–136. [PubMed: 16464905]
26. Miyakoshi N, Richman C, Kasukawa Y, Linkhart T, Baylink D, Mohan S. Evidence that IGF-binding protein-5 functions as a growth factor. J Clin Invest. 2001; 107(1):73–81. [PubMed: 11134182]
27. Bradley EW, Oursler MJ. Osteoclast culture and resorption assays. Methods Mol Biol. 2008; 455:19–35. [PubMed: 18463808]
28. Xing W, Kim J, Wergedal J, Chen ST, Mohan S. Ephrin B1 regulates bone marrow stromal cell differentiation and bone formation by influencing TAZ transactivation via complex formation with NHERF1. Mol Cell Biol. 2010; 30(3):711–721. [PubMed: 19995908]
29. Wergedal JE, Ackert-Bicknell CL, Tsaih SW, Sheng MH, Li R, Mohan S, Beamer WG, Churchill GA, Baylink DJ. Femur mechanical properties in the F2 progeny of an NZB/B1NJ x RF/J cross are regulated predominantly by genetic loci that regulate bone geometry. J Bone Miner Res. 2006; 21(8):1256–1266. [PubMed: 16869724]
30. Mohan S, Kutilek S, Zhang C, Shen HG, Kodama Y, Srivastava AK, Wergedal JE, Beamer WG, Baylink DJ. Comparison of bone formation responses to parathyroid hormone(1–34), (1–31), and (2–34) in mice. Bone. 2000; 27(4):471–478. [PubMed: 11033441]
31. Xing W, Singgih A, Kapoor A, Alarcon CM, Baylink DJ, Mohan S. Nuclear factor-E2-related factor-1 mediates ascorbic acid induction of osterix expression via interaction with antioxidant-responsive element in bone cells. J Biol Chem. 2007; 282(30):22052–22061. [PubMed: 17510056]
32. Linares GR, Xing W, Govoni KE, Chen ST, Mohan S. Glutaredoxin 5 regulates osteoblast apoptosis by protecting against oxidative stress. Bone. 2009; 44(5):795–804. [PubMed: 19442627]
33. Peng H, Chen S, Wergedal J, Polo J, Yee J, Lau K, Baylink D. Development of an MFG-based retroviral vector system for secretion of high levels of functionally active human BMP4. Mol Ther. 2001; 4(2):95–104. [PubMed: 11482980]
34. Edderkaoui B, Baylink DJ, Beamer WG, Wergedal JE, Porte R, Chaudhuri A, Mohan S. Identification of mouse Duffy antigen receptor for chemokines (Darc) as a BMD QTL gene. Genome Res. 2007; 17(5):577–585. [PubMed: 17416748]
35. Xing W, Archer TK. Upstream stimulatory factors mediate estrogen receptor activation of the cathepsin D promoter. Mol Endocrinol. 1998; 12(9):1310–1321. [PubMed: 9731700]
36. Linares GR, Xing W, Burghardt H, Baumgartner B, Chen ST, Ricart W, Fernandez-Real JM, Zorzano A, Mohan S. Role of Diabetes and Obesity Related Protein (DOR) in the Regulation of Osteoblast Differentiation. Am J Physiol Endocrinol Metab. 2011
37. Levaot N, Simoncic PD, Dimitriou ID, Scotter A, La Rose J, Ng AH, Willett TL, Wang CJ, Janmohamed S, Grynpas M, Reichenberger E, Rottapel R. 3BP2-deficient mice are osteoporotic with impaired osteoblast and osteoclast functions. J Clin Invest. 2011; 121(8):3244–3257. [PubMed: 21765218]
38. Hayashi D, Tamura A, Tanaka H, Yamazaki Y, Watanabe S, Suzuki K, Sentani K, Yasui W, Rakugi H, Isaka Y, Tsukita S. Deficiency of Claudin-18 Causes Paracellular H(+) Leakage, Up-regulation of Interleukin-1β, and Atrophic Gastritis in Mice. Gastroenterology. 2012; 142(2):292–304. [PubMed: 22079592]
39. Ramasamy I. Recent advances in physiological calcium homeostasis. Clin Chem Lab Med. 2006; 44(3):237–273. [PubMed: 16519596]
40. Niimi T, Nagashima K, Ward JM, Minoo P, Zimonjic DB, Popescu NC, Kimura S. claudin-18, a novel downstream target gene for the T/EBP/NKX2.1 homeodomain transcription factor, encodes

lung- and stomach-specific isoforms through alternative splicing. Mol Cell Biol. 2001; 21(21): 7380–7390. [PubMed: 11585919]

41. Yano K, Imaeda T, Niimi T. Transcriptional activation of the human claudin-18 gene promoter through two AP-1 motifs in PMA-stimulated MKN45 gastric cancer cells. Am J Physiol Gastrointest Liver Physiol. 2008; 294(1):G336–343. [PubMed: 18032479]
42. Jovov B, Van Itallie CM, Shaheen NJ, Carson JL, Gambling TM, Anderson JM, Orlando RC. Claudin-18: a dominant tight junction protein in Barrett's esophagus and likely contributor to its acid resistance. Am J Physiol Gastrointest Liver Physiol. 2007; 293(6):G1106–1113. [PubMed: 17932229]
43. Hamazaki Y, Itoh M, Sasaki H, Furuse M, Tsukita S. Multi-PDZ domain protein 1 (MUPP1) is concentrated at tight junctions through its possible interaction with claudin-1 and junctional adhesion molecule. J Biol Chem. 2002; 277(1):455–461. [PubMed: 11689568]
44. Itoh M, Furuse M, Morita K, Kubota K, Saitou M, Tsukita S. Direct binding of three tight junction-associated MAGUKs, ZO-1, ZO-2, and ZO-3, with the COOH termini of claudins. J Cell Biol. 1999; 147(6):1351–1363. [PubMed: 10601346]
45. Roh MH, Makarova O, Liu CJ, Shin K, Lee S, Laurinec S, Goyal M, Wiggins R, Margolis B. The Maguk protein, Pals1, functions as an adapter, linking mammalian homologues of Crumbs and Discs Lost. J Cell Biol. 2002; 157(1):161–172. [PubMed: 11927608]
46. Asagiri M, Takayanagi H. The molecular understanding of osteoclast differentiation. Bone. 2007; 40(2):251–264. [PubMed: 17098490]
47. Yamazaki Y, Tokumasu R, Kimura H, Tsukita S. Role of claudin-species specific dynamics in reconstitution and remodeling of the zonula occludens. Mol Biol Cell. 2011
48. Islas S, Vega J, Ponce L, González-Mariscal L. Nuclear localization of the tight junction protein ZO-2 in epithelial cells. Exp Cell Res. 2002; 274(1):138–148. [PubMed: 11855865]
49. Jaramillo BE, Ponce A, Moreno J, Betanzos A, Huerta M, Lopez-Bayghen E, Gonzalez-Mariscal L. Characterization of the tight junction protein ZO-2 localized at the nucleus of epithelial cells. Exp Cell Res. 2004; 297(1):247–258. [PubMed: 15194440]
50. Betanzos A, Huerta M, Lopez-Bayghen E, Azuara E, Amerena J, González-Mariscal L. The tight junction protein ZO-2 associates with Jun, Fos and C/EBP transcription factors in epithelial cells. Exp Cell Res. 2004; 292(1):51–66. [PubMed: 14720506]
51. Huerta M, Muñoz R, Tapia R, Soto-Reyes E, Ramírez L, Recillas-Targa F, González-Mariscal L, López-Bayghen E. Cyclin D1 is transcriptionally down-regulated by ZO-2 via an E box and the transcription factor c-Myc. Mol Biol Cell. 2007; 18(12):4826–4836. [PubMed: 17881732]
52. Traweger A, Lehner C, Farkas A, Krizbai IA, Tempfer H, Klement E, Guenther B, Bauer HC, Bauer H. Nuclear Zonula occludens-2 alters gene expression and junctional stability in epithelial and endothelial cells. Differentiation. 2008; 76(1):99–106. [PubMed: 17973926]
53. Thorleifsson G, Holm H, Edvardsson V, Walters GB, Styrkarsdottir U, Gudbjartsson DF, Sulem P, Halldorsson BV, de Vegt F, d'Ancona FC, den Heijer M, Franzson L, Christiansen C, Alexandersen P, Rafnar T, Kristjansson K, Sigurdsson G, Kiemeney LA, Bodvarsson M, Indridason OS, Palsson R, Kong A, Thorsteinsdottir U, Stefansson K. Sequence variants in the CLDN14 gene associate with kidney stones and bone mineral density. Nat Genet. 2009; 41(8): 926–930. [PubMed: 19561606]
54. Kim JH, Jin HM, Kim K, Song I, Youn BU, Matsuo K, Kim N. The mechanism of osteoclast differentiation induced by IL-1. J Immunol. 2009; 183(3):1862–1870. [PubMed: 19587010]
55. Yao Z, Xing L, Boyce BF. NF-kappaB p100 limits TNF-induced bone resorption in mice by a TRAF3-dependent mechanism. J Clin Invest. 2009; 119(10):3024–3034. [PubMed: 19770515]
56. Doty SB. Morphological evidence of gap junctions beetween bone cells. Calcif Tissue Int. 2001; 33:509–512. [PubMed: 6797704]
57. Lecanda F, Warlow PM, Sheikh S, Furlan F, Steinberg TH, Civitelli R. Connexin43 deficiency causes delayed ossification, craniofacial abnormalities, and osteoblast dysfunction. J Cell Biol. 2000; 151(4):931–944. [PubMed: 11076975]
58. Ilvesaro J, Tuukkanen J. Gap-junctional regulation of osteoclast function. Crit Rev Eukaryot Gene Expr. 2003; 13(2–4):133–146. [PubMed: 14696962]

59. Saitou M, Furuse M, Sasaki H, Schulzke JD, Fromm M, Takano H, Noda T, Tsukita S. Complex phenotype of mice lacking occludin, a component of tight junction strands. Mol Biol Cell. 2000; 11(12):4131–4142. [PubMed: 11102513]

60. Xu J, Kausalya PJ, Phua DC, Ali SM, Hossain Z, Hunziker W. Early embryonic lethality of mice lacking ZO-2, but Not ZO-3, reveals critical and nonredundant roles for individual zonula occludens proteins in mammalian development. Mol Cell Biol. 2008; 28 (5):1669–1678. [PubMed: 18172007]

61. Umeda K, Ikenouchi J, Katahira-Tayama S, Furuse K, Sasaki H, Nakayama M, Matsui T, Tsukita S, Furuse M. ZO-1 and ZO-2 independently determine where claudins are polymerized in tight-junction strand formation. Cell. 2006; 126(4):741–754. [PubMed: 16923393]

62. Hou J, Shan Q, Wang T, Gomes AS, Yan Q, Paul DL, Bleich M, Goodenough DA. Transgenic RNAi depletion of claudin-16 and the renal handling of magnesium. J Biol Chem. 2007; 282(23): 17114–17122. [PubMed: 17442678]

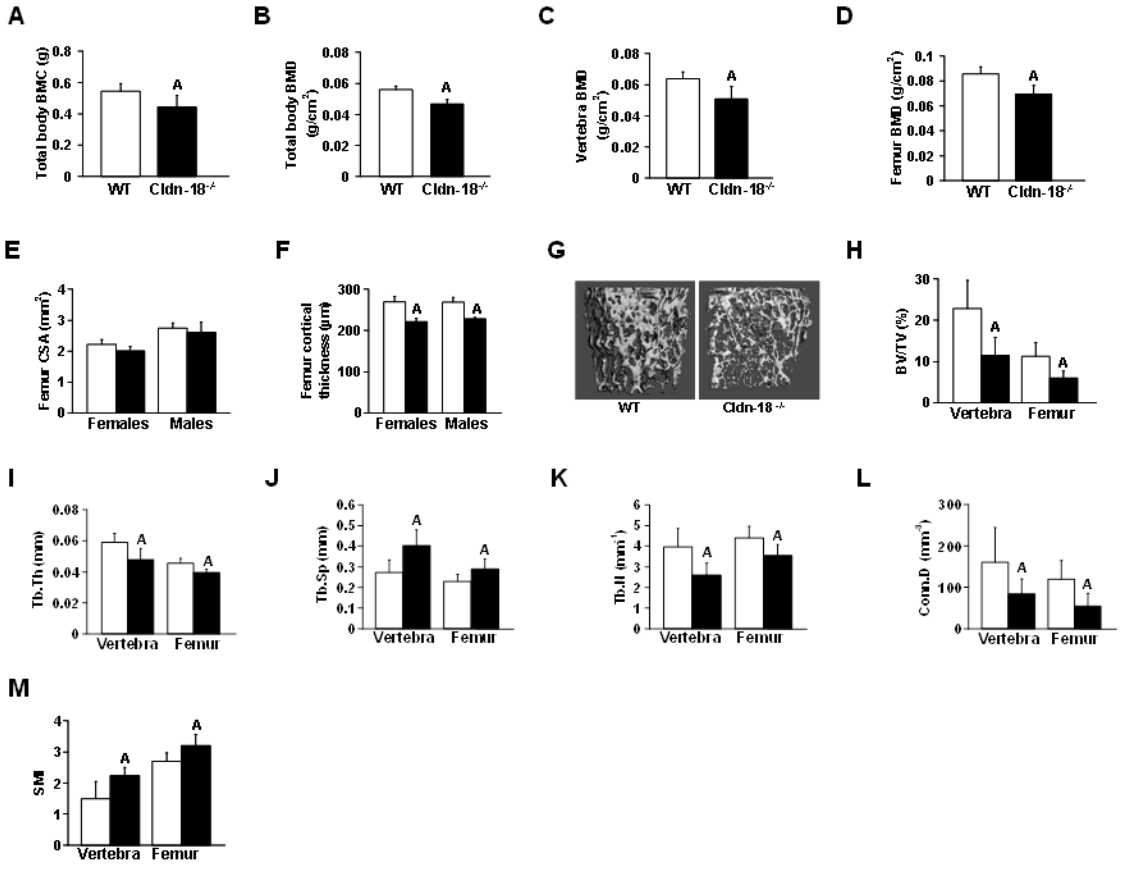

Fig. 1.

Cldn-18 $^{-/-}$ mice exhibit reduced bone mineral density. (A) Total body BMC, (B) total body BMD, (C) vertebra BMD, and (D) femur BMD as determined by DXA in WT and *Cldn-18* $^{-/-}$ mice at 26 weeks of age (genders combined). (n=8/group); A=P < 0.01 vs. WT littermates. (E) Cross sectional area (CSA) and (F) cortical thickness at femur mid diaphysis in WT (open bars) and *Cldn-18* $^{-/-}$ mice (filled bars) at 26 weeks. (n=3–5/group); A=P < 0.05 vs. WT littermates. (G) μCT image of distal femur metaphysis from 26 week old WT and *Cldn-18* $^{-/-}$ mice. (H–M) Quantitative measurements of trabecular bone structure of L5 vertebra and distal femur metaphysis (genders combined). (H) % Trabecular bone volume (BV/TV %) (I) Trabecular thickness (Tb.Th) (J) Trabecular spacing (Tb.Sp) (K) Trabecular number (Tb.N) (L) Connectivity density (Conn.D) (M) Structure model index (SMI). (n=8/group); A=P < 0.05 vs. WT littermates.

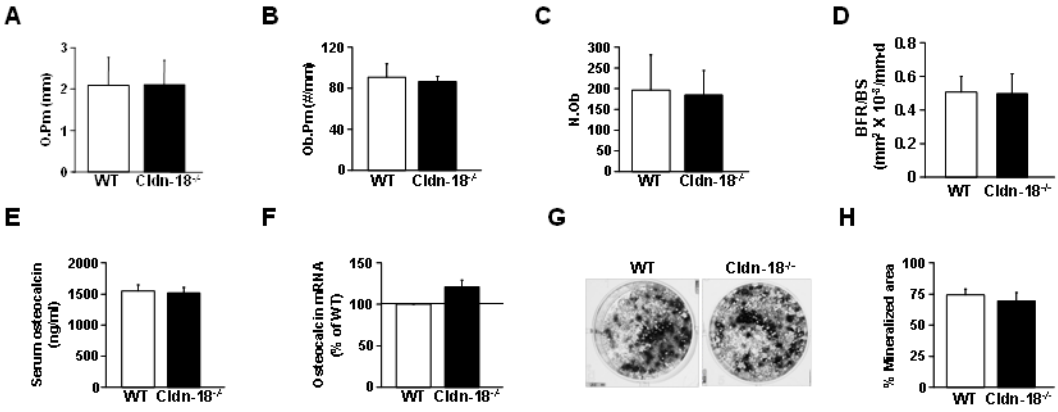

Fig. 2.

Bone formation is unaffected by Cldn-18 deficiency. (A–D) Bone formation parameters measured at the trabecular bone of secondary spongiosa of the proximal tibia in wild type and *Cldn-18* $^{-/-}$ mice at 4 weeks of age. (A) Osteoid surface (O.Pm) (B) Osteoblast surface (Ob.Pm) (C) Osteoblast number (N.Ob) (D) Bone formation rate (BFR). (n=10–14/group). (E) Serum osteocalcin levels in WT and *Cldn-18* $^{-/-}$ mice. (n=10–14/group). (F) Osteocalcin gene expression in the femurs of WT and *Cldn-18* $^{-/-}$ mice as determined by real time RT-PCR. (n=14/group). (G) Mineralized nodule formation in WT and *Cldn-18* $^{-/-}$ mice as determined by Alizarin red staining. (H) Quantitative mineralization area as measured by Osteomeasure system. (n=5/group).

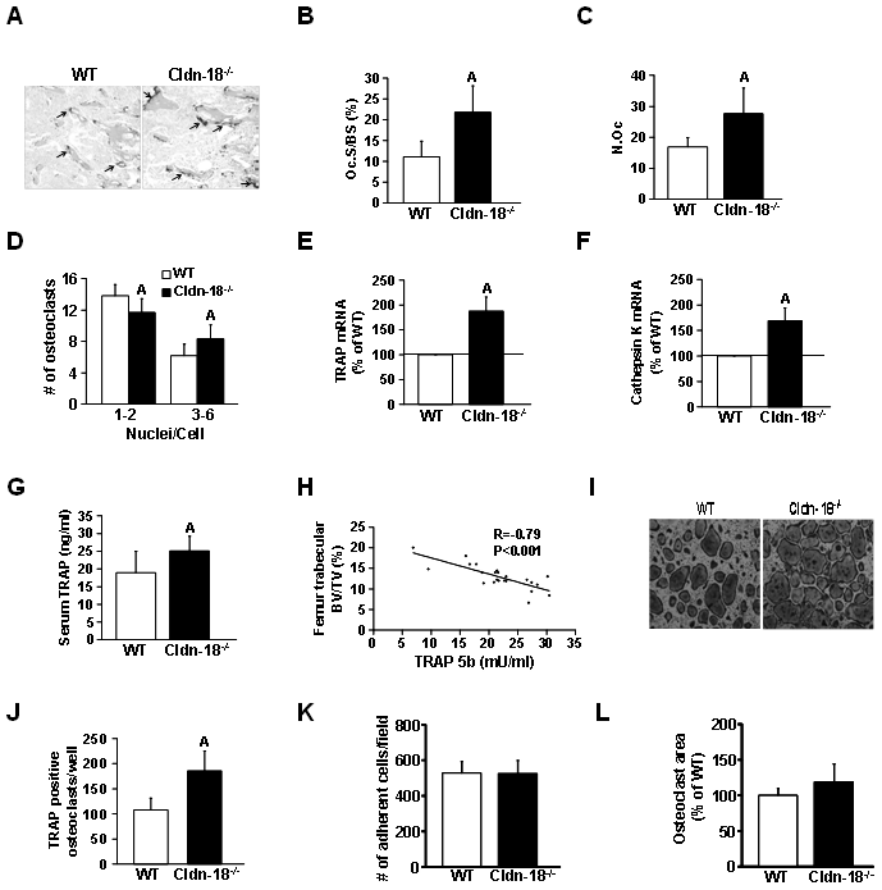

Fig. 3.

Disruption of Cldn-18 increases bone resorption and osteoclast formation.

(A) TRAP staining of osteoclasts in trabecular bone at secondary spongiosa of the proximal tibia in WT and *Cldn-18* $^{-/-}$ mice at 4 weeks of age. Sections were counterstained with methyl green. Arrows denote representative osteoclasts. (B) Osteoclast surface (Oc.S/BS) and (C) osteoclast number (N.Oc) in WT and *Cldn-18* $^{-/-}$ mice at 4 weeks of age. (n=14/group); A=P < 0.05 vs. WT. (D) Number of nuclei per osteoclast in WT and *Cldn-18* $^{-/-}$ mice at 4 weeks of age. (n=6/group); A= P < 0.05 vs. WT. (E) TRAP and (F) Cathepsin K gene expression in the femurs of WT and *Cldn-18* $^{-/-}$ mice as determined by real time RT-PCR. (n=14/group); A=P < 0.05 vs. WT. (G) Serum TRAP5b levels in WT and *Cldn-18* $^{-/-}$ mice. (n=10–14/group); A=P < 0.05 vs. WT. (H) Negative correlation between femur trabecular bone volume and Trap5b in *Cldn-18* $^{-/-}$ mice. (I) *In vitro* osteoclast differentiation of BMMs derived from WT and *Cldn-18* $^{-/-}$ mice cultured in the presence of MCSF (50 ng/ml) and RANKL (100 ng/ml). (J) Quantification of multinucleated TRAP positive cells. (n=8/group); A=P < 0.01 vs. WT. (K) Quantitative evaluation of MCSF-mediated preosteoclast adhesion (60 minutes) to culture dishes. Data represents mean ± SD of 4 fields per well (n=3/group). (L) Quantitation of size of multinucleated TRAP positive cells. BMMs-derived from WT and *Cldn-18* $^{-/-}$ mice (n=3/group) were treated with MCSF and RANKL for 6 days and stained for TRAP activity. The multinucleated osteoclast area was measured using Image Pro Version 4.5 software (Media Cybernetics, Bethesda, MD).

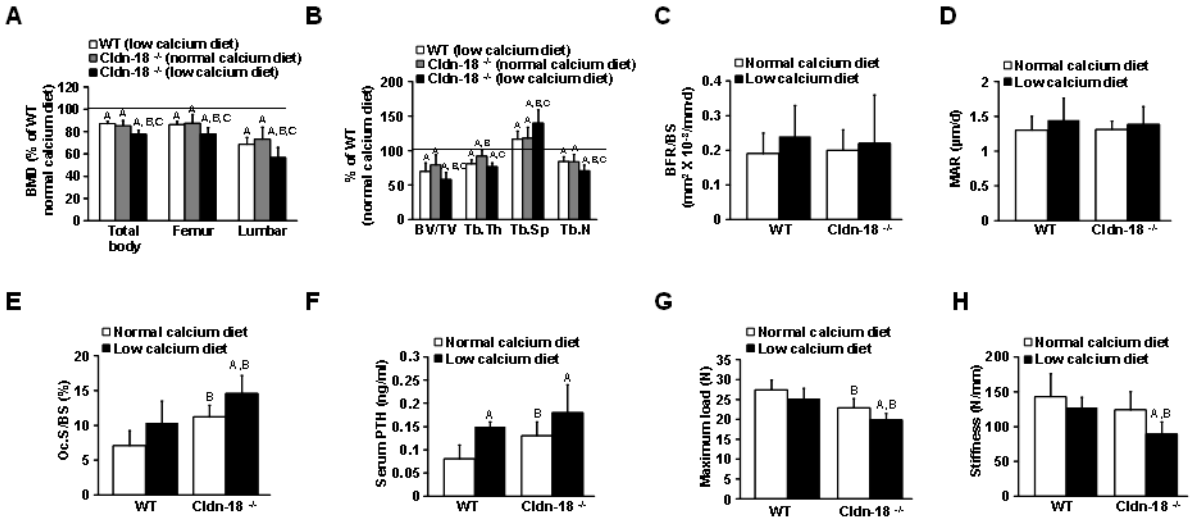

Fig. 4.

Effect of calcium deficiency in *Cldn-18* $^{-/-}$ mice. Sixteen week old WT and *Cldn-18* $^{-/-}$ mice were subjected to a normal calcium or low calcium diet for 2 weeks. (A) Total body BMD, femur BMD, and lumbar BMD as determined by DXA (n=14/group). (B) Quantitative measurements of trabecular bone structure of L5 vertebra as determined by μCT analysis. (n=14/group). (C) Bone formation rate (BFR) at the trabecular bone of secondary spongiosa of distal femur (n=6/group). (D) Mineral apposition rate (MAR) at the trabecular bone of secondary spongiosa of distal femur (n=6/group). (E) Osteoclast surface (Oc.S/BS) (n=6/group) of the trabecular bone at secondary spongiosa of the distal femur. (F) Serum PTH levels in WT and *Cldn-18* $^{-/-}$ mice fed a normal calcium or low calcium diet (n=6/group). (G) Maximum load in the femurs of WT and *Cldn-18* $^{-/-}$ female mice as determined by 3-point bending. (n=6/group). (H) Stiffness of the femur in WT and *Cldn-18* $^{-/-}$ female mice. (n=6/group). (A–B) A=P < 0.05 vs WT (normal calcium diet), B=P < 0.05 vs. WT (low calcium diet), and C=P < 0.05 vs. *Cldn-18* $^{-/-}$ (normal calcium diet). (C–H) A=P < 0.05 vs. corresponding control group fed normal calcium diet and B=P < 0.05 vs. corresponding WT mice.

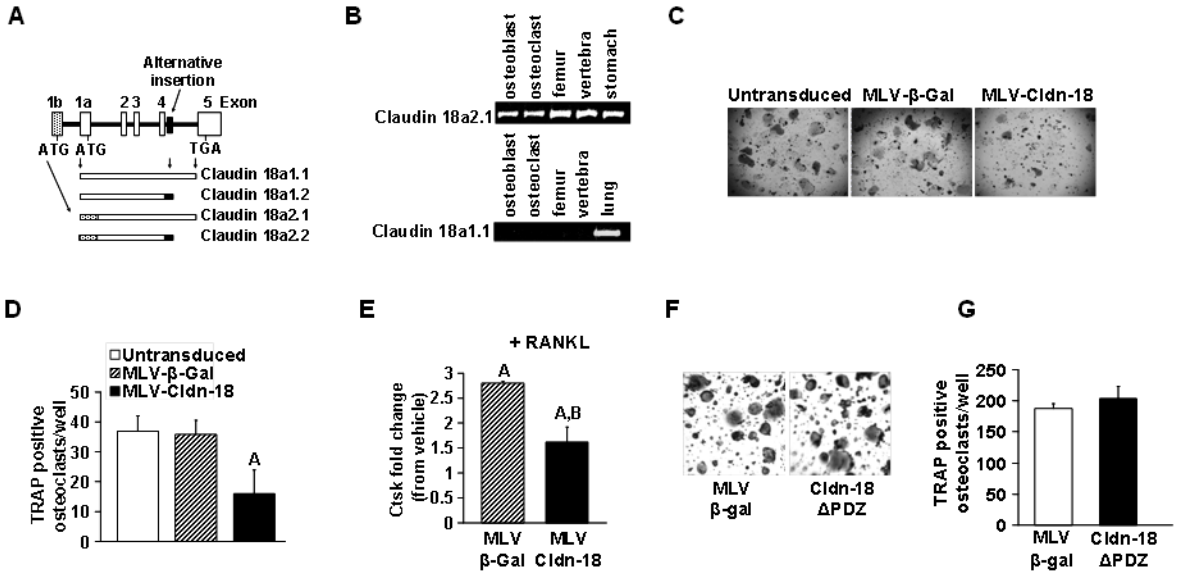

Fig. 5.

Cldn-18 variant 18a2.1 is expressed in bone and influences osteoclast formation. (A) Schematic representation of four types of Cldn-18 transcripts. Organization of exons and introns and predictions for production of four types of transcripts are shown. The alternatively inserted 12-bp sequence after exon 4 is depicted with a black box. (B) Expression of Claudin 18a2.1 and Claudin 18a1.1 as measured by RT-PCR. Cldn 18a1.2 and 18a2.2 transcript was not detected by RT-PCR (data not shown). (C) *In vitro* osteoclast differentiation of untransduced RAW264.7 cells, or RAW264.7 cells containing MLV-β-Gal or MLV-Cldn-18 cultured in the presence of RANKL (100 ng/ml). (D) Quantification of multinucleated TRAP positive cells. (n=5–8/group); A=P < 0.01 vs. untransduced or MLV-β–Gal. (E) Real-time RT-PCR analysis of Cathepsin K expression in MLV-β-Gal and MLV-Cldn-18 RAW264.7 cells treated with RANKL (30 ng/ml) for 24 hours. (n=4/group); A=P < 0.05 vs. vehicle and B=P < 0.05 vs. MLV-β-Gal. (F) *In vitro* osteoclast differentiation of RAW264.7 cells containing MLV-β-Gal or MLV-ΔPDZ Cldn-18 (cytoplasmic tail containing PDZ binding motif deleted) cultured in the presence of RANKL (100 ng/ml). (G) Quantification of multinucleated TRAP positive cells in RANKL-induced RAW264.7 cells overexpressing β-Gal or MLV-ΔPDZ Cldn-18. (n=8/group).

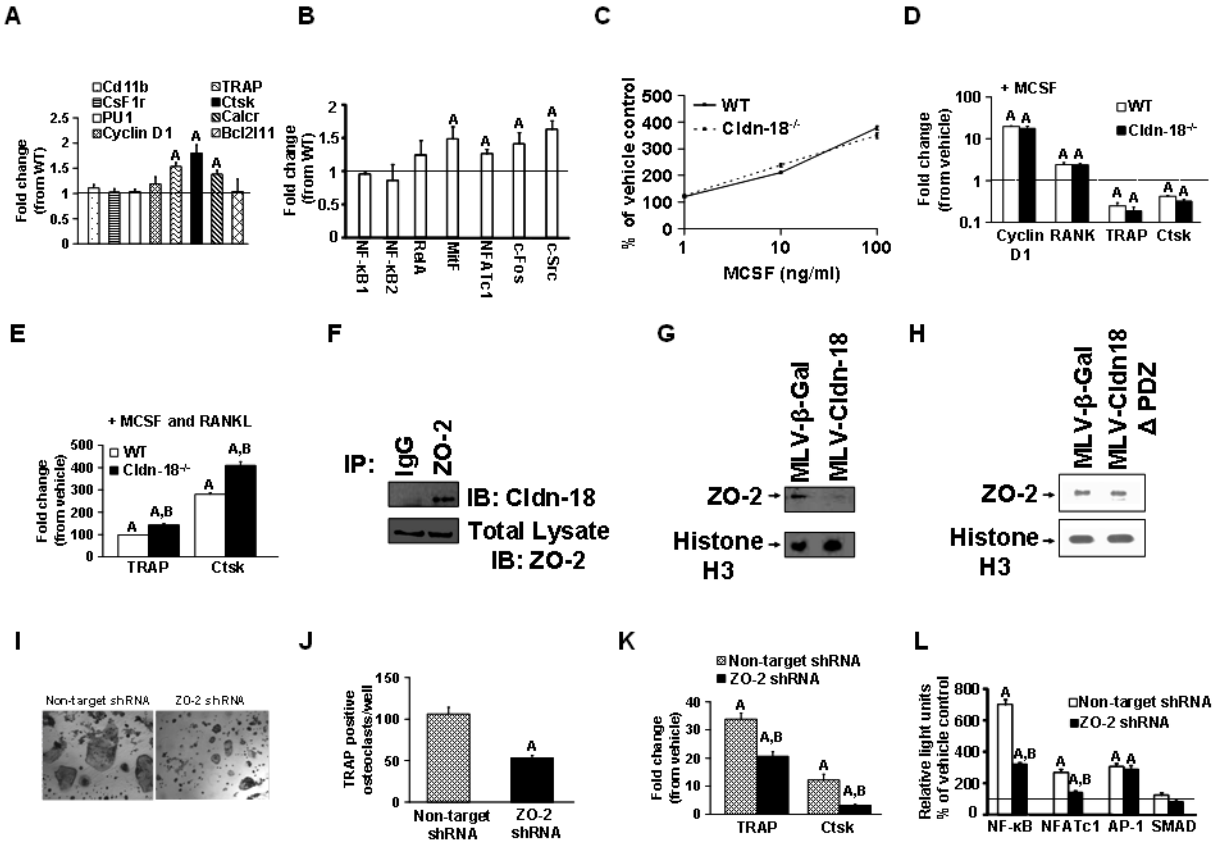

Fig. 6.

Cldn-18 regulates RANKL signaling in osteoclasts. (A) Real time RT-PCR analysis of osteoclast precursor and differentiation markers in whole femurs (including bone marrow) of 3 week old WT and *Cldn-18* $^{-/-}$ mice. (n=8/group); A=P < 0.05 vs. WT. (B) Real time RT-PCR analysis of transcription factors known to be involved in the osteoclast differentiation pathway. RNA was extracted from whole femurs (including bone marrow) of 3 week old WT and *Cldn-18* $^{-/-}$ mice. (n=8/group); A=P < 0.05 vs. WT. (C) BMM precursor proliferation (n=8/group). (D) Real time RT-PCR analysis of Cyclin D1, RANK, TRAP, and Ctsk expression in WT and *Cldn- 18* $^{-/-}$ BMMs treated with MCSF (30 ng/ml) for 24 hours. (n=4/group); A=P < 0.05 vs. vehicle. (E) Real-time RT-PCR analysis of TRAP and Ctsk expression in WT and *Cldn-18* $^{-/-}$ BMMs treated with MCSF (30 ng/ml) and RANKL (100 ng/ml) for 72 hours. (n=4/group); A=P < 0.05 vs. vehicle and B=P < 0.05 vs. WT. (F) Whole cell lysates from MLV-Cldn-18 RAW264.7 cells were immunoprecipitated with antibody specific to ZO-2 and immunoblotted with Cldn-18. An aliquot from the immunoprecipitation was probed with ZO-2 and served as a loading control. (G) Immunoblot analysis of ZO-2 levels in nuclear fractions of MLV-β–Gal and MLV-Cldn-18 RAW264.7 cells cultured with RANKL (30 ng/ml) for 6 hours. Histone H3 served as an internal control. (H) Immunoblot analysis of ZO-2 levels in nuclear fractions of MLV-β–Gal and MLV-Cldn-18 ΔPDZ (cytoplasmic tail containing PDZ binding motif deleted) RAW264.7 cells cultured with RANKL (30 ng/ml) for 6 hours. Histone H3 served as an internal control. (I) *In vitro* osteoclast differentiation of RAW264.7 cells transduced with non-target shRNA or ZO-2 shRNA cultured with RANKL (100 ng/ml). (J) Quantification of multinucleated TRAP positive cells. (n=8/group); A=P < 0.01 vs. non-target shRNA. (K) Real-time RT-PCR analysis of TRAP and Ctsk expression in non-target shRNA and ZO-2 shRNA cells treated with RANKL (100 ng/ml) for 24 hours. (n=4/group); A=P < 0.05 vs.

vehicle and B=P < 0.05 vs. non-target shRNA. (L) Cignal ™ Lenti reporter (luc) transcriptional activity in non-target shRNA and ZO-2 shRNA cells incubated in the presence of RANKL for 12 hours (n=8/group); A=P <0.01 vs. vehicle and B=P < 0.05 vs. non-target shRNA.